Phosphomolybdic Acid-Catalyzed Oxidative Degradation of Waste Starch: A New Strategy For Handling The Pulping Wastewater

Yongzhen Qiao
Nanjing Forestry University
Weisheng Yang
Nanjing Forestry University
Xiu Wang
Nanjing Forestry University
Liang Jiao
Nanjing Forestry University
Yiqin Yang
Nanjing Forestry University
Shumei Wang
Nanjing Forestry University
Huiyang Bian
Nanjing Forestry University
Hongqi Dai (hgdhq@njfu.edu.cn)
Nanjing Forestry University

Research Article

Keywords: OCC waste paper, Waste starch, Phosphomolybdic acid, Reducing sugar, Recycle utilization

Posted Date: February 25th, 2021

DOI: https://doi.org/10.21203/rs.3.rs-231180/v1

Abstract

When old corrugated cardboard (OCC) is returned to the paper mill for repulping and reuse, the starch, which is added to the paper surface as a reinforcement agent, is dissolved into the pulping process water. Most of the OCC pulping wastewater is recycled to save precious water resources; however, during the water recycling process, the accumulation of dissolved starch stimulates microbial reproduction, which causes poor water quality and putrid odor. This problem seriously affects the stability of the papermaking process and product quality. In this study, phosphomolybdic acid ($H_3PMo_{12}O_{40}$, abbreviated as PMo_{12}) was utilized to oxidatively degrade the waste starch present in papermaking wastewater to monosaccharides, realizing the resource utilization of waste starch. The results showed that the optimized yield of total reducing sugar (73.54 wt%) and glycolic acid (11.05 wt%)was achieved at 145 °C with 30 wt% PMo_{12}, which is equivalent to 84.59 wt% starch recovered from wastewater. In addition, the regeneration of the reduced PMo_{12} was realized applying a potential of 1 V for 2 h. Overall, this study has theoretical significance and potential application value for resource utilization of waste starch in OCC pulping process and cleaner management of OCC waste paper.

Introduction

In the production of corrugated paper and liner paper, starch is often used as a paper surface enhancer because of its low cost, environmental protection, and degradability (Li et al. 2013; Wang C 2020). However, when the old corrugated cardboard (OCC) waste paper made from corrugated cardboard boxes and test liner is returned to the paper mill for pulping and papermaking, most of the starch on the paper surface is dissolved into the water during dissociation of waste paper fibers. The starch, which accumulates abundantly in the papermaking system, has a serious effect on the papermaking production, particularly regarding environmental impact, stability of the system operation, and product quality. Simultaneously, the accumulated starch also causes proliferation of microorganisms(Zhu et al. 2017), which results in rot and smell and further deterioration of the production system, the environment, and product quality (Lin et al. 2020; Miao et al. 2012). Generally, anaerobic fermentation is used for the production of biogas, wastewater treatment, and energy recovery (Chaterjee et al. 2019; Sun et al. 2011). According to the China Paper Association report in 2019(Association 2020), the total production of corrugated cardboard containers in China is 44 million tons, accounting for 40.9% of total paper production. Commonly, starch consumption is approximately 40–60 kg for every ton of paper fibers; the total consumption of starch based on the above reports is 1.76–2.64 million tons every year, which is equivalent to 303,000~455,000 ha of fields (the average yield of corn starch is 5800 kg/ha)(Lin et al. 2020). This implies the wasting of a large amount of food.

Polyoxometalates (POMs) are polymetallic oxygen cluster compounds consisting of a metal–oxygen octahedron, which have become a research hotspot in many fields due to their low corrosivity and environmental protection (Guo et al. 2019; Wang and Yang 2015). POMs are considered as water-soluble metal oxide nanoparticles (Du et al. 2017; Wu et al. 2016), and have both acidic and redox characteristics, as well as unique "pseudo-liquid phase" characteristics (Long et al. 2010). Therefore, it is more efficient

for catalyzing the reactions. These compounds can be redox active in solution by electrochemical oxidation because of its multielectron property, while their anion structure is preserved (Chen et al. 2019; Glass et al. 2016). POMs have been used for the degradation of biomass (Albert et al. 2012; Bosco et al. 2010; Zhang et al. 2012). Thus, Liu et al. used phosphomolybdic acid ($H_3PMo_{12}O_{40}$, abbreviated as PMo_{12}) to degrade biomass such as cellulose and starch into small molecules of sugars and organic acids (Liu et al. 2016). Tian et al. hydrolyzed cellulose with phosphotungstic acid ($H_3PW_{12}O_{40}$) at 180 °C for 120 min. The glucose yield was more than 50% with 92.3% glucose selectivity, and few byproducts were obtained (Tian et al. 2010). Starch and cellulose are high molecular polymers formed by dehydration of glucose units (Buléon et al. 1998; Goodman 2020). Therefore, POMs can be used to hydrolyze starch to produce reducing sugar (RS) (Mamman et al. 2008; Mua and Jackson 1997) and glycolic acid(Zhang et al. 2012), having demonstrated excellent electrochemical performance on the degradation of biomass.

Herein, recycled waste starch (WS) in OCC pulping process water was oxidized and degraded using PMo_{12}. The influencing factors, namely, reaction temperature, time, and PMo_{12} usage, on the production of RS and glycolic acid from WS were evaluated. Furthermore, the recycling performance of PMo_{12} after electrooxidation regeneration was analyzed. The feasibility of turning WS to RS and glycolic acid using PMo_{12} was studied. The specific experimental process is presented in Fig. 1. This work is expected to provide a theoretical guidance and application reference for realizing resource utilization of WS in the OCC pulping process water and developing clean papermaking production.

Materials And Methods

Materials

WS from OCC pulping process water was provided by Nine Dragons Paper Co., Ltd (Taicang, China). PMo_{12} was supplied by Shanghai Aladdin Chemicals Co., Ltd. (Shanghai, China). Glucose (AR), cesium chloride (CsCl, AR), and diethyl ether (AR) were purchased from Sinopharm Chemical Reagent Co., Ltd. (Shanghai, China). 3, 5-Dinitrosalicylic acid (DNS) was prepared according to a previous work (Adeogun et al. 2019; Miller 1959).

Curve determination of glucose standard solution

Glucose (1 g) was added to a volumetric flask, and deionized (DI) water was added to obtain a volume of 1 L. From this solution, which was labeled as standard solution, 0, 0.2, 0.4, 0.6, 0.8, and 1.0 mL was taken respectively, supplemented with DI water to 1 mL, and 2 mL DNS was added. After reaction in boiling water bath for 2 min, the solution was placed in an ice water bath. Finally, the reaction solution was fixed to 15 mL. The absorbance of the mixture was measured using a UV757CRT Model spectrophotometer at 540 nm (Miller 1959; Tian et al. 2010). The DNS reagent reacted with RS to form 3-amino-5-nitrosalicylic acid. The product was brownish red under boiling condition, and the color was proportional to the RS content in a certain concentration range.

Separation of waste starch in OCC pulping wastewater

The wastewater from the multi-disc thickener in the OCC re-pulping was filtrated by Busher funnel with 325 mesh firstly. Then, the filtration was centrifuged at 4500 rpm for 20 min using a high-speed centrifuge. The supernatants were subsequently placed in a dialysis bag with MW-CO 8000–12000(D).Then, a water-soluble organic solution (waste starch and water-soluble organic matter) without the inorganic substances was obtained. The concentration of WS was measured with amylase by HPLC(Lin et al. 2020).

Hydrothermal reaction of WS with PMo_{12}

WS was easily oxidized and degraded by PMo_{12} under hydrothermal conditions. The hydrothermal treatment was conducted in a 250 mL three-port flask reactor equipped with a stirring device and a condenser. A WS solution was prepared and transferred to the reactor, to which a certain amount of PMo_{12} was added. Then, the mixture was heated in an oil bath to the desired temperature with a stirring speed of 300 r/min. The effect of hydrothermal temperature was investigated at 140 °C, 145 °C, 150 °C, 155 °C and 160 °C, and the PMo_{12} dosage based on WS was investigated from 20 to 80 wt% for 60, 120, 180, and 240 min. Under direct heating, the solution gradually changed from yellow to dark blue. Then, 5 mL of sample was taken every 60 min for standby sampling and diluted to 1 mmol/L, and the reduction degree of PMo_{12} was determined simultaneously by absorbance spectrophotometry at 700 nm. To this aim, the standard curve of the reduction degree versus absorbance of PMo_{12} was obtained by titrating a PMo_{12} solution with a $KMnO_4$ standard solution (0.01 mol/L).

Determination of total reducing sugar content after the hydrothermal reaction

The PMo_{12} present in the mixture after the hydrothermal reaction was removed. After addition of a slight excess CsCl, a precipitate was immediately generated. The upper solution was cleared by centrifugation. Then, the supernatants were filtered through a filter with a pore size of 0.22 μm, and the filtered liquid contained the total reducing sugar (TRS). Then, a mixture containing 2 mL of DNS reagent and 1 mL of filtrate was heated in a boiling water bath for 2 min, and 12 mL of DI water was added after the mixture was cooled down to room temperature. The color intensity of the mixture was measured in a UV757CRT Model spectrophotometer at a wavelength of 540 nm. The concentration of TRS was calculated according to a standard curve obtained from the concentration of glucose using Equation 1.

$$\mathrm{TRS\ yield(wt\%)} = \frac{c \times v}{m} \times 100\% \qquad (1)$$

where *c* denotes the concentration of TRS, *v* is the volume of TRS, and *m* represents the WS mass.

The concentrations of glycolic acid, 5-hydroxymethylfurfural (5-HMF), levulinic acid, and formic acid were quantitatively determined by an external standard method; then, their quantities in the liquid products of hydrolysis were calculated according to the liquid yields. The concentration of the liquid products in the

filtrate was determined by HPLC using an Aminex BioRad-HPX-87H column and a refractive index detector. The mobile phase was 5 mM H_2SO_4, the flow rate was 0.6 mL/min, and the column temperature was 55 °C. Two parallel assays were performed for each experiment.

Electrochemical oxidation of PMo_{12}

The electrolysis cell was composed of a high-density graphite plate with a serpentine groove, a Nafion 115 membrane, a silicone gasket, a platinum sheet as cathode, and graphite felt as anode. The bipolar plates of the cell were high-density graphite plates with a serpentine flow channel 2 mm wide, 5 mm deep, and 50 mm long (the total geometry projected area of the channel was 1 cm^2), which is schematically illustrated in Fig. 2. The graphite felt was pretreated with concentrated HNO_3 and H_2SO_4 in a 1:3 volumetric ratio at 50 °C for 30 min. Then, the graphite felt was washed with DI water until the pH of the wash water became neutral, dried at 80 °C, and cut into pieces with the thickness of 5 mm and width of 2 mm. These graphite felt electrodes were filled into the channel of the anode (Liu et al. 2014a). Diethyl ether was added to the dark blue waste starch–PMo_{12} solution after the hydrothermal reaction. PMo_{12} was extracted to the upper layer after full shaking (Okuhara 2002; Tian et al. 2010). When the diethyl ether was completely volatilized using rotary evaporator, PMo_{12} was dissolved in DI water. The PMo_{12} solution was then pumped into the anode, and the phosphoric acid aqueous solution (1 mol/L) was pumped into the cathode side of the cell. A potential of 1 V was applied by an electrochemical workstation for electrooxidation. From the solution, a sample was collected every 1 h and diluted to 1 mmol/L for analysis of the reduction degree of PMo_{12} by spectrophotometry.

Results And Discussion

Analysis of the factors influencing the oxidative degradation of WS

The factors determining the oxidative degradation of WS include reaction time, temperature, pH of the reaction system, and concentration of reactants (Girisuta et al. 2007; Mukherjee et al. 2016). We conducted single-factor experiments to select the three main factors, i.e., reaction temperature, PMo_{12} dosage, and reaction time, in a targeted manner, and obtained the optimal process conditions for determination of the TRS yield.

First, the standard curve of this experiment was adjusted to zero with the color reaction solution of DI water as control, and the standard working curve was drawn with the mass fraction of glucose as the abscissa and the absorbance as the ordinate (Fig. 3a). The regression equation was $y = 0.0185x + 0.1074$ ($R^2 = 0.9980$), where R^2 is the correlation coefficient and defines the feasibility of the method and the degree of linear relationship. Generally, $R^2 > 0.99$ ensures an appropriate limit of error. The DNS reagent was used to determine the TRS content in the experiment.

Effect of reaction temperature on TRS and glycolic acid yield

Here, the measured concentration of WS was about 5 g/L by HPLC. Thus, in all experiments, 5 g/L, 100 mL of WS filtrate was applied. 20 wt% of PMo_{12} and 120 min of reaction time were applied in this part. As shown in Fig. 3b, the TRS yield increased and then decreased with increasing the reaction temperature. The highest TRS yield of 62.98 wt% was obtained at 145 °C; the highest yield of glycolic acid was 16.45 wt% at 160 °C. Then, with further increasing the reaction temperature to 160 °C, the yield rapidly decreased to 33.63 wt%, which was 46.60% lower than that at 145 °C. On the contrary, the increase of glycolic acid was 4.92 wt% from 145 °C to 160 °C. Therefore, it can be concluded that the reaction temperature was an important factor that restricts the conversion of starch into RS, and had a great influence on the TRS yield, meaning that starch could not be fully hydrolyzed to RS at lower temperature. However, as the temperature increased, the oxidation of PMo_{12} played a major role, and the oxidative degradation of RS was violent. In acidic solution at a high temperature, RS was the intermediate substance in the process of WS degradation, and was easily degraded in acid medium to produce insoluble humins and other byproducts (Yu et al. 2017). Basically, to prevent ineffective degradation of starch, the optimization reaction temperature is 145 °C, the sum of TRS and glycolic was 74.91 wt%.

Effect of PMo_{12} dosage on TRS and glycolic acid yield

Apart from the effects of temperature and time, the dosage of PMo_{12} also had a significant influence on the hydrolysis of WS to glucose. The acidity of PMo_{12} accelerates the hydrolysis of WS, and the oxidation contributes to the cleavage of chemical bonds of WS, driving the reaction forward. Different TRS yields were obtained by changing the PMo_{12} dosage (20, 30, 50, and 80 wt%) at 145 °C for 120 min. For a dosage of 20 wt%, most degradation was observed, and the TRS yield was only 62.98 wt% (Fig. 3c). Fortunately, the TRS yield increased rapidly to 73.54 wt% and 75.83 wt%, and the glycolic yield was 11.05 wt% to 12.99 wt% when the PMo_{12} dosage was 30 to 50 wt%, respectively. However, the TRS yield did not increase significantly with further increasing the PMo_{12} dosage. Hence, from the perspective of environmental protection and economy, the optimal reaction condition was 30 wt% PMo_{12}, which afforded a TRS yield of 73.54 wt% and 11.04 wt% yield of glycolic acid.

Effect of reaction time on TRS and glycolic acid yield

With the optimized reaction temperature and PMo_{12} dosage in hands, which were 145 °C and 30 wt%, respectively, the TRS yield was explored at different reaction times. We found that the TRS yield increased first and then decreased with the reaction time (Fig. 3d). This was because the RS was further degraded under high temperature and acidic conditions. Simultaneously, organic degradation products such as glycolic acid, 5-HMF and formic acid were generated. With increasing the reaction time, the C–C bond cleavage effect of PMo_{12} increased(Khenkin and Neumann 2008), which favored the production of levulinic acid and formic acid. Although the TRS yield was only 0.57 wt% higher at 180 min than at 120 min, the reaction time increased by 60 min. Consequently, the TRS yield was reduced. The optimized TRS yield of 73.54 wt% was obtained for 120 min reaction time. In conclusion, the optimal conditions for the

catalytic hydrothermal process to achieve a TRS yield of 73.54 wt% were 145 °C reaction temperature, 30 wt% PMo_{12}, and 120 min reaction time.

Mechanism of the PMo_{12}-catalyzed oxidative degradation of starch

As shown in Table 1, the main product of starch degradation using PMo_{12} was TRS, and a small number of byproducts (e.g., glycolic acid, 5-HMF, formic acid, and levulinic acid) were detected by HPLC(Deng et al. 2012).

Table 1 Products analysis of oxidation degradation of WS by PMo_{12}

Conditions (T/°C)	Main products				
	TRS (wt%)	Glucose (wt%)	Glycolic acid(wt%)	5-HMF (wt%)	Formicacid(wt%)
140	46.57 ± 2.67	26.02 ± 2.53	5.34 ± 2.77	0.19 ± 1.08	0
145	62.98 ± 3.11	31.39 ± 2.87	11.93 ± 2.43	0.43 ± 2.13	0
150	58.76 ± 2.32	28.72 ± 2.43	14.18 ± 2.45	0.88 ± 2.19	0.83 ± 2.07
155	48.43 ± 3.42	23.46 ± 3.11	15.12 ± 2.54	1.42 ± 3.41	1.63 ± 1.99
160	33.63 ± 2.67	13.91 ± 2.87	16.45 ± 2.77	1.90 ± 3.15	2.49 ± 2.16

Notes: 5 g/L WS, 20 wt% PMo_{12} (PMo_{12}/WS mass ratio), 120 min reaction time.

Fig. 4a, b display a plausible reaction mechanism for the PMo_{12}-catalyzed oxidative degradation of starch. The branched macro-molecule amylopectin and the linear macromolecule amylose, which consists of crystalline and amorphous lamellae of starch, form a semi-crystalline structure in the starch granule(Farias et al. 2020). It means that starch contains a large number of α-1, 4 glycosidic bonds and fewer α-1, 6 glycosidic bonds. The –O–H, C–O–C, and C–C bonds in starch molecular chain are cleaved due to the strong Brønsted acidity and oxidation properties of PMo_{12}(Li et al. 2012; Liu et al. 2014a; Liu et al. 2014b). Thus, H^+ ions penetrate into the starch molecule in the hydrothermal reaction process, cleaving the α-1, 4 and α-1, 6 glycosidic bonds. Moreover, the amorphous region of starch likely undergoes cleavage reaction affording the hydrolysate RS, which is mainly composed of monosaccharides. In the oxidative degradation stage of PMo_{12} and starch macromolecules, a hydrogen bond is formed between a free –OH in the starch molecule and an O atom of Mo–O in PMo_{12} (Fig. 4a). Meanwhile, a proton and an electron are provided to PMo_{12} by the starch molecule. Then, an O–H covalent bond is formed between free –OH and Mo–O at high temperature. On the one hand, the glucose

is converted to 5-HMF by isomerization and dehydration. Furthermore, part of 5-HMF continues to generate formic acid and levulinic acid via decarboxylation. On the other hand, the glycolaldehyde and erythrose are oxidative intermediate byproduct from the retro-aldol fragmentation of glucose, and are continuously oxidized to glycolic acid(Zhang et al. 2012) (Fig. 4b). The Mo^{6+} cation is simultaneously reduced to Mo^{5+} in PMo_{12} to form molybdenum blue via electron transfer(Dolbecq et al. 2010), with the concomitant solution color change to blue. Fortunately, the structure of PMo_{12} is not destroyed (Chen et al. 2019; Glass et al. 2016; He and Yao 2006). Due to the oxidative property of PMo_{12}, a number of degradation products can be further oxidized to compounds such as 5-HMF, formic acid, and levulinic acid.

PMo_{12} regeneration properties

The long-term cycle stability of a catalyst is an important index to evaluate its performance, especially in industrial application. Therefore, the recovery rate of PMo_{12} after three cycles and its influence on the TRS yield were investigated. The absorbance of PMo_{12} at 700 nm was used to determine the reduction degree because both variables have a linear relationship (Fig. 5a). The absorbance curve of PMo_{12} in a wavelength range from 400 to 900 nm under different hydrothermal reaction times is shown in Fig. 5b. Upon increasing the reaction time from 60 min to 240 min, the reduction degree of PMo_{12} also increased, which indicates that WS was degraded. The reduction degree of molybdenum blue (reductive PMo_{12}) decreased gradually in the process of electrooxidation, being gradually oxidized and converted to oxidative PMo_{12} (Fig. 5c)(Yang et al. 2019). Fig. 5d demonstrates that the TRS yield changed between the first and third cycle of PMo_{12} treatment, decreasing from 69.56 wt% for the first cycle to 58.32 wt% for the third cycle. Nevertheless, the recovery rate of PMo_{12} after the third cycle was still 80.76% of the initial value. The decreased catalytic performance of recovered PMo_{12} may be due to organics adsorption by PMo_{12}, which affects the oxidative degradation of WS. Fortunately, a good level of PMo_{12} recycling performance was still maintained.

The color change of PMo_{12} solution during the redox process is illustrated in Fig. 6. Under the hydrothermal reaction, the WS–PMo_{12} mixture changed from yellow to dark blue (Fig. 6a and Fig. 6b), indicating the reduction of PMo_{12} to molybdenum blue. The Mo^{6+} cation in PMo_{12} is reduced by electrons from WS, and the reduction degree of PMo_{12} increases. The reduction degree of a POM is defined as the average number of electrons (in moles) that are transferred from the biomass to one mole of the POM anion(Liu et al. 2016; Zhao et al. 2020). A CHI660E electrochemical workstation was utilized to oxidize a molybdenum blue solution at a constant voltage of 1.0 V in the electrolysis, which was lower than the standard potential of water electrolysis (1.23 V)(Weng and Chen 2015). During electrolysis, Mo^{5+} in molybdenum blue was oxidized to Mo^{6+} at the anode. Simultaneously, the molybdenum blue was converted to oxidative PMo_{12}. The color of the solution turned back to yellow, and WS was oxidized and degraded (Fig. 6c). A H^+ from WS was transferred to the cathode, generating hydrogen.

Conclusions

A large amount of dissolved WS pollutants are accumulated in pulping wastewater during the process of repulping and reuse of OCC waste paper. To solve this problem, we investigated the degradation of WS by the green catalytic oxidant PMo_{12}, and the mechanism of the reaction was explored. WS was effectively oxidized and degraded to high value-added RS. During the hydrothermal reaction, at 145 °C, a PMo_{12} dosage of 30 wt%, and a reaction time of 120 min, the TRS yield from WS reached 73.54 wt% and glycolic acid (11.05 wt%), which was equivalent to 84.59 wt% of starch recovered from OCC pulping wastewater. Molybdenum blue can be oxidized to oxidative PMo_{12} by electrolysis, realizing the recycle and reuse of PMo_{12}. The present study on the oxidative degradation of starch by PMo_{12} has theoretical significance and potential application value for resource utilization of WS in OCC pulping process and cleaner management of OCC waste paper.

Declarations

Acknowledgements The author thanks the support from the National Natural Science Foundation of China (No.3177030417) and the Major Science and Technology Plan Project of Jiangsu Province (BE2018129). The authors also thank Zhina Lian (Nanjing Forestry University) for the HPLC tests, and Rui Liu (Nanjing IPE Institute of Green Manufacturing Industry) for the linguistic assistance.

Author Contributions Yongzhen Qiao: Conceptualization, Formal analysis, Methodology, Validation, Investigation, Writing - Original Draft, Writing - Review & Editing. Weisheng Yang: Investigation, Methodology, Formal analysis. Xiu Wang: Language. Liang Jiao: Resources. Huiyang Bian: Language, Resources. Yiqin Yang: Methodology, Resources. Shumei Wang: Resources. Hongqi Dai: Conceptualization, Supervision, Funding acquisition.

Availability of data and materials Availability of data and materials has been provided.

Ethics approval and consent to participate Not applicable.

Consent for publication Not applicable.

Competing interests The authors declare that they have no competing interests.

References

1. Adeogun AI, Agboola BE, Idowu MA, Shittu TA (2019) $ZnCl_2$ Enhanced Acid Hydrolysis of Pretreated Corncob for Glucose Production: Kinetics, Thermodynamics and Optimization Analysis. J Bioresour Bioprod 4:149-158 doi:10.12162/jbb.v4i3.003
2. Albert J, Woelfel R, Boesmann A, Wasserscheid PJE, ence E (2012) Selective oxidation of complex, water-insoluble biomass to formic acid using additives as reaction accelerators. Energy Environ Sci 5:7956-7962 doi:10.1039/C2EE21428H

3. Association C, P. (2020) 2019 Annual Report of China's Paper Industry. Pap Biomater:70-80 doi:10.12103/j.issn.2096-2355.2020.03.007
4. Bosco M, Rat DS, Dupré N, Hasenknopf B, Lacôte E, Malacria M, Rémy DP, Kovensky J, Thorimbert S, Wadouachi AJC (2010) Lewis-Acidic Polyoxometalates as Reusable Catalysts for the Synthesis of Glucuronic Acid Esters under Microwave Irradiation. ChemSusChem 3:1249-1252 doi:10.1002/cssc.201000218
5. Buléon A, Colonna P, Planchot V, Ball S (1998) Starch granules: structure and biosynthesis. Int J Biol Macromol 23:85-112 doi:10.1016/S0141-8130(98)00040-3
6. Chaterjee PK, Neogi S, Saha S, Jeon BH, Dey A (2019) Low pH treatment of starch industry effluent with bacteria from leaf debris for methane production. Water Environ Res 91:377-385 doi:10.1002/wer.1033
7. Chen X, Huang P, Zhu X, Zhuang S, Zhu H, Fu J, Nissimagoudar AS, Li W, Zhang X, Zhou LJNH (2019) Keggin-type polyoxometalate cluster as an active component for redox-based nonvolatile memory. Nanoscale Horiz 4:697-704 doi:10.1039/C8NH00366A
8. Deng W, Zhang Q, Wang Y (2012) Polyoxometalates as efficient catalysts for transformations of cellulose into platform chemicals. Dalton Trans (Cambridge, England : 2003) 41:9817-9831 doi:10.1039/c2dt30637a
9. Dolbecq A, Dumas E, Mayer C, Mialane P (2010) ChemInform Abstract: Hybrid Organic-Inorganic Polyoxometalate Compounds: From Structural Diversity to Applications. Chem Rev 110:6009-6048 doi:10.1021/cr1000578
10. Du X, Liu W, Zhang Z, Mulyadi A, Brittain A, Gong J, Deng Y (2017) Low-Energy Catalytic Electrolysis for Simultaneous Hydrogen Evolution and Lignin Depolymerization. ChemSusChem 10:847-854 doi:10.1002/cssc.201601685
11. Farias FdAC, Moretti MMdS, Costa MS, BordignonJunior SE, Cavalcante KB, Boscolo M, Gomes E, Franco CML, Silva Rd (2020) Structural and physicochemical characteristics of taioba starch in comparison with cassava starch and its potential for ethanol production. Ind Crops Prod 157:112825 doi:10.1016/j.indcrop.2020.112825
12. Girisuta B, Janssen LPBM, Heeres HJ (2007) Kinetic Study on the Acid-Catalyzed Hydrolysis of Cellulose to Levulinic Acid. Ind Eng Chem Res 46:1696-1708 doi:10.1021/ie061186z
13. Glass EN, Fielden J, Huang Z, Xiang X, Musaev DG, Lian T, Hill CLJIC (2016) Transition metal substitution effects on metal-to-polyoxometalate charge transfer. Inorg Chem 55:4308-4319 doi:10.1021/acs.inorgchem.6b00060
14. Goodman BA (2020) Utilization of waste straw and husks from rice production: A review. J Bioresour Bioprod 5:143-162 doi:10.1016/j.jobab.2020.07.001
15. Guo K, Guan Q, Xu J, Tan W (2019) Mechanism of Preparation of Platform Compounds from Lignocellulosic Biomass Liquefaction Catalyzed by Bronsted Acid: A Review. J Bioresour Bioprod 4:202-213 doi:10.12162/jbb.v4i4.009

16. He T, Yao J (2006) Photochromism in composite and hybrid materials based on transition-metal oxides and polyoxometalates. Prog Mater Sci 51:810-879 doi:10.1016/j.pmatsci.2005.12.001
17. Khenkin AM, Neumann RJJotACS (2008) Oxidative C–C bond cleavage of primary alcohols and vicinal diols catalyzed by $H_5PV_2Mo_{10}O_{40}$ by an electron transfer and oxygen transfer reaction mechanism. J Am Chem Soc 130:14474-14476 doi:10.1021/ja8063233
18. Li J, Ding D-J, Deng L, Guo Q-X, Fu Y (2012) Catalytic Air Oxidation of Biomass-Derived Carbohydrates to Formic Acid. ChemSusChem 5:1313-1318 doi:10.1002/cssc.201100466
19. Li X, Zhao C, Zhang H, Han W (2013) Preparation of Enzymatic Starch and Effect of Surface Sizing on Properties of the Paper. Adv Mater Res 848:321-324 doi:10.4028/scientific.net/AMR.848.321
20. Lin L, Yang J, Ni S, Wang X, Bian H, Dai H (2020) Resource utilization and ionization modification of waste starch from the recycling process of old corrugated cardboard paper. J Environ Manage 271:111031 doi:10.1016/j.jenvman.2020.111031
21. Liu W, Cui Y, Du X, Zhang Z, Chao Z, Deng YJE, Science E (2016) High efficiency hydrogen evolution from native biomass electrolysis. Energy Environ Sci 9:467-472 doi:10.1039/C5EE03019F
22. Liu W, Mu W, Deng Y (2014a) High-Performance Liquid-Catalyst Fuel Cell for Direct Biomass-into-Electricity Conversion. Angew Chem, Int Ed 53:13558-13562 doi:10.1002/anie.201408226
23. Liu W, Mu W, Liu M, Zhang X, Cai H, Deng Y (2014b) Solar-induced direct biomass-to-electricity hybrid fuel cell using polyoxometalates as photocatalyst and charge carrier. Nat Commun 5:3208 doi:10.1038/ncomms4208
24. Long D-L, Tsunashima R, Cronin L (2010) Polyoxometalates: Building Blocks for Functional Nanoscale Systems. Angew Chem, Int Ed Engl 49:1736-1758 doi:10.1002/anie.200902483
25. Mamman AS, Lee J-M, Kim Y-C, Hwang IT, Park N-J, Hwang YK, Chang J-S, Hwang J-S (2008) Furfural: Hemicellulose/xylosederived biochemical. Biofuels, Bioprod Biorefin 2:438-454 doi:10.1002/bbb.95
26. Miao Q, Huang L, Chen L (2012) Advances in the Control of Dissolved and Colloidal Substances Present in Papermaking Processes: A Brief Review. BioResources 8:1431-1455 doi:10.15376/biores.8.1.1431-1455
27. Miller GL (1959) Use of Dinitrosalicylic Acid Reagent for Determination of Reducing Sugar. Anal Chem 31:426-428 doi:10.1021/ac60147a030
28. Mua J, Jackson D (1997) Relationship Between Functional Attributes and Molecular Structures of Amylose and Amylopectin Fractions from Corn Starch. J Agric Food Chem 45:3848-3854 doi:10.1021/jf9608783
29. Mukherjee A, Dumont M-JeJI, Research EC (2016) Levulinic acid production from starch using microwave and oil bath heating: a kinetic modeling approach. Ind Eng Chem Res 55:8941-8949
30. Okuhara T (2002) Water-Tolerant Solid Acid Catalysts. Chem Rev 102:3641-3665 doi:10.1021/cr0103569

31. Sun L, Wan S, Yu Z, Wang Y, Wang S (2011) Anaerobic biological treatment of high strength cassava starch wastewater in a new type up-flow multistage anaerobic reactor. Bioresour Technol 104:280-288 doi:10.1016/j.biortech.2011.11.070
32. Tian J, Wang J, Zhao S, Jiang C, Zhang X, Wang X (2010) Hydrolysis of cellulose by the heteropoly acid $H_3PW_{12}O_{40}$. Cellulose 17:587-594 doi:10.1007/s10570-009-9391-0
33. Wang C GH, Chen X, Ni S, Liu N, Dai H (2020) Study on the Preparation and Application Performance of Nano Starch. Journal of Qilu University of Technology 34:28-34 doi:10.16442/j.cnki.qlgydxxb.2020.04.005
34. Wang S-S, Yang G-Y (2015) Recent Advances in Polyoxometalate-Catalyzed Reactions. Chemical reviews 115:4893-4962 doi:10.1021/cr500390v
35. Weng S, Chen X (2015) A hybrid electrolyzer splits water at 0.8 V at room temperature. Nano Energy 19:138-144 doi:10.1016/j.nanoen.2015.11.018
36. Wu W, Liu W, Mu W, Deng Y (2016) Polyoxymetalate liquid-catalyzed polyol fuel cell and the related photoelectrochemical reaction mechanism study. J Power Sources 318:86-92 doi:10.1016/j.jpowsour.2016.03.074
37. Yang W, Du X, Liu W, Tricker AW, Dai H, Deng Y (2019) Highly Efficient Lignin Depolymerization via Effective Inhibition of Condensation during Polyoxometalate-Mediated Oxidation. Energy Fuels 33:6483-6490 doi:10.1021/acs.energyfuels.9b01175
38. Yu IKM, Tsang D, Yip A, Chen S, Wang L, Ok YS, Poon CS (2017) Catalytic Valorization of Starch-Rich Food Waste into Hydroxymethylfurfural (HMF): Controlling Relative Kinetics for High Productivity. Bioresour Technol 237:222-230 doi:10.1016/j.biortech.2017.01.017
39. Zhang J, Liu X, Sun M, Ma X, Han Y (2012) Direct Conversion of Cellulose to Glycolic Acid with a Phosphomolybdic Acid Catalyst in a Water Medium. ACS Catalysis 2:1698-1702 doi:10.1021/cs300342k
40. Zhao Y, Wang T, Wang H, Lu S, Wang Y, Zhao M, Lu X, Li B (2020) Study on POM assisted electrolysis for hydyrogen and ammonia production. Int J Hydrogen Energy doi:10.1016/j.ijhydene.2020.07.147
41. Zhu H, Qin L, Hu Y, Wei D, Hai Z, Li A, Xie X, Han C (2017) Occurrence and transformations of carbon, nitrogen, and phosphorus related to particle size fraction of sweet potato starch wastewater during hydrolytic acidification processes. Environ Sci Pollut Res 24:20717-20724 doi:10.1007/s11356-017-9724-8

Figures

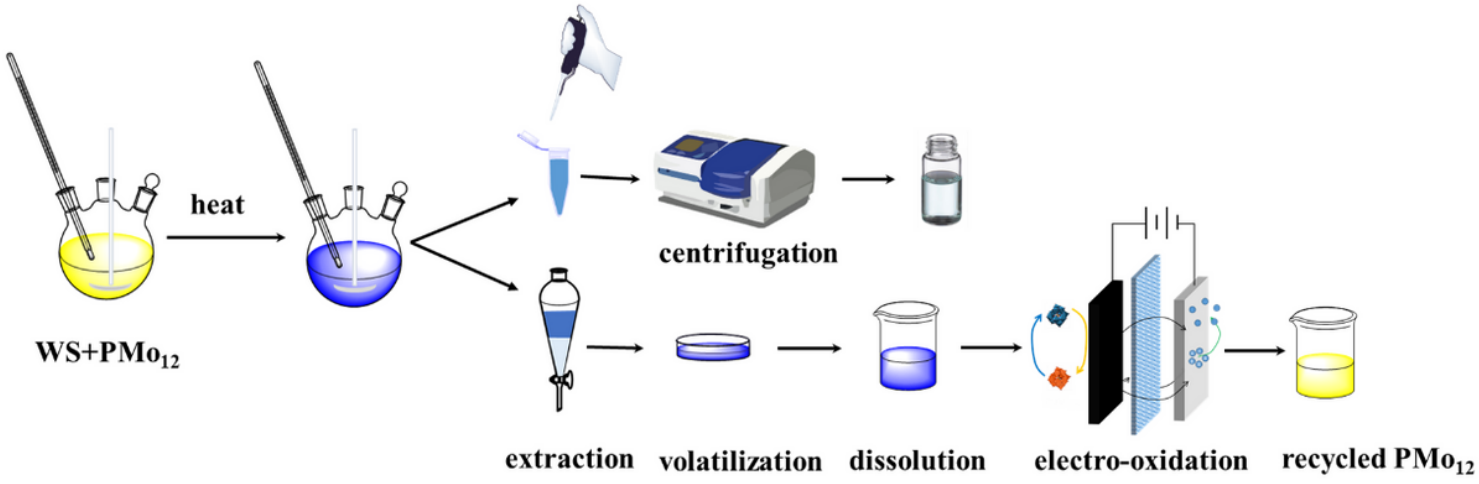

Figure 1

Schematic diagram of the oxidative degradation of the WS using PMo12 and electro-oxidation cycle of PMo12.

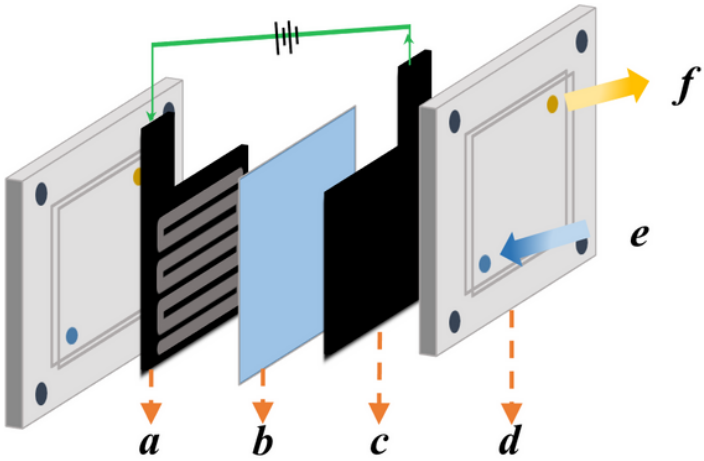

a. Graphite serpentine groove with Pt sheet
b. Nafion 115
c. Graphite felt
d. Polymethyl methacrylate
e. Reduced PMo_{12} solution
f. Oxidized PMo_{12} solution

Figure 2

Structure of the electrolysis cell.

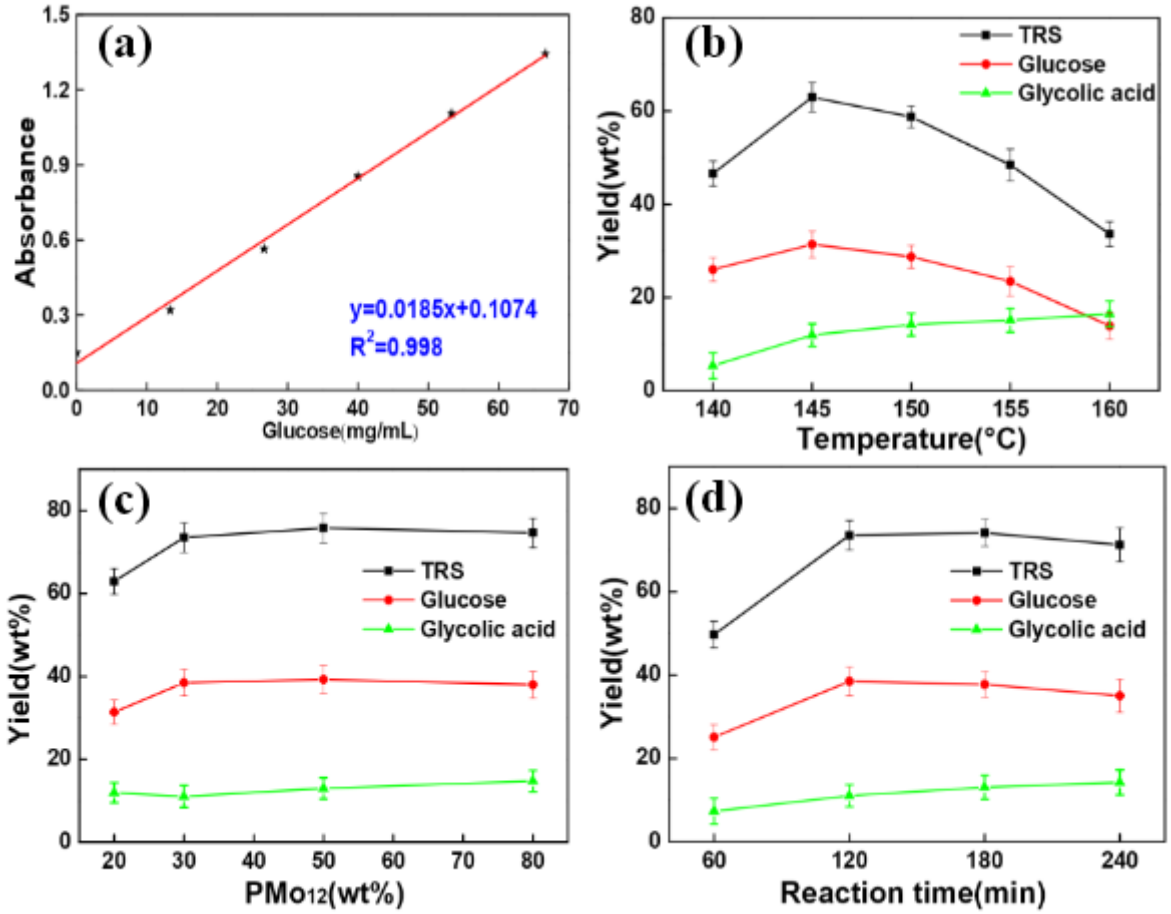

Figure 3

a Glucose standard curve; The influence of b Reaction temperature; c Dosage of PMo12; d Reaction time on hydrothermal oxidation.

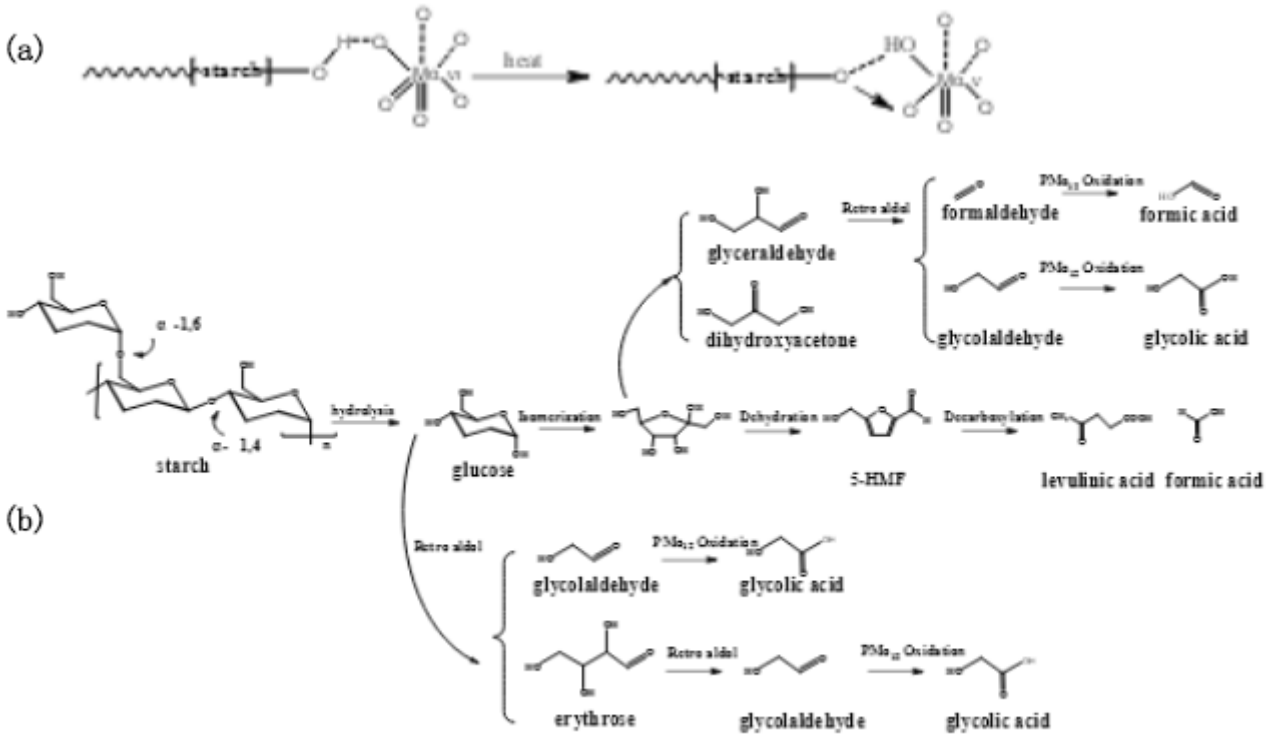

Figure 4

The proposed reaction pathway in the degradation of WS with PMo12

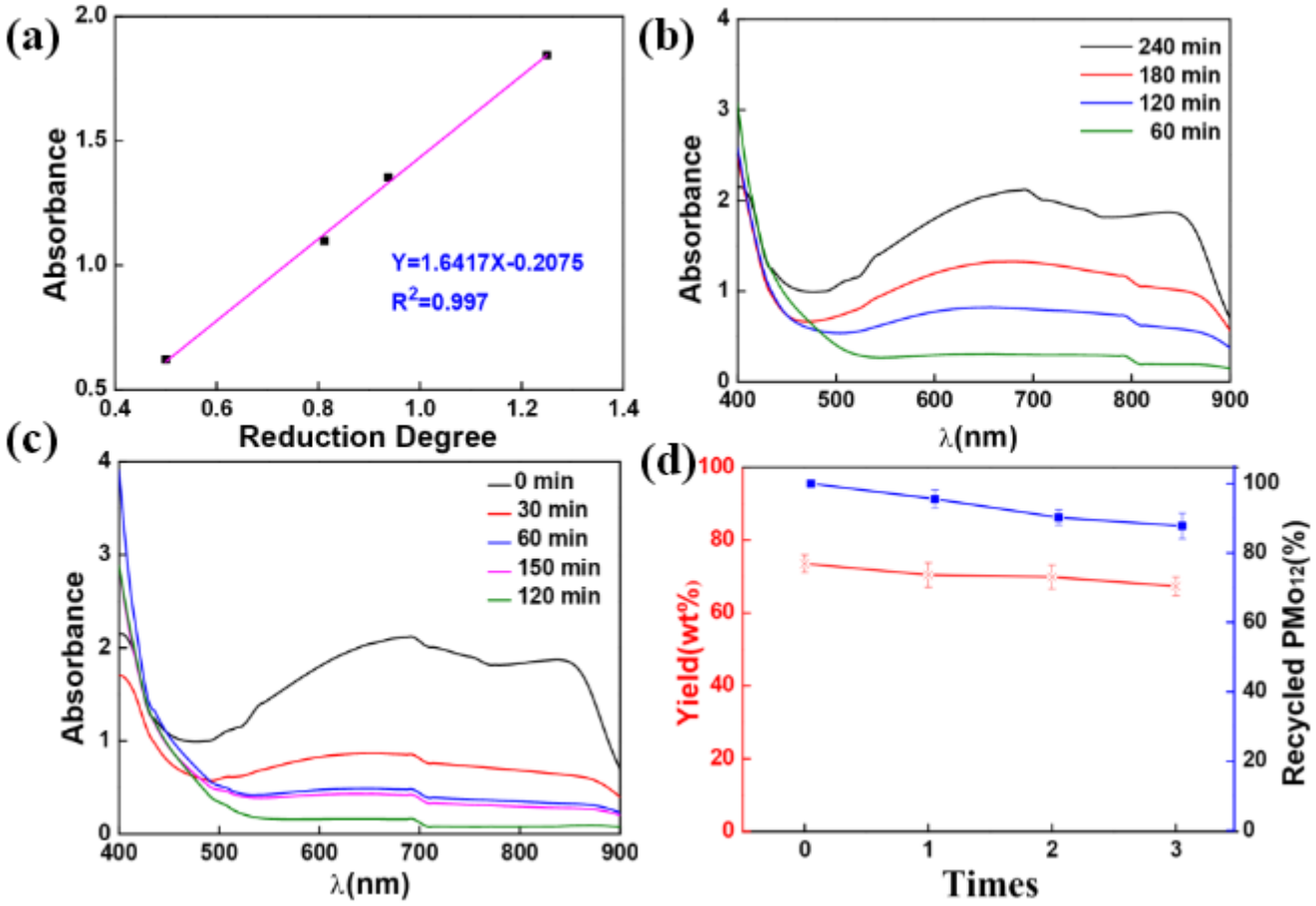

Figure 5

Cyclic performance test of PMo12 with a Calibration curve for PMo12 solution with different reduction degrees; b UV-Vis spectrum of WS-PMo12 solution during the hydrothermal degradation process (diluted to 1 mmol/L); c UV-Vis spectrum of PMo12 solution during electro-oxidation (diluted to 1 mmol/L); d Relationship between recycling recovery of PMo12, TRS yield and cycle times.

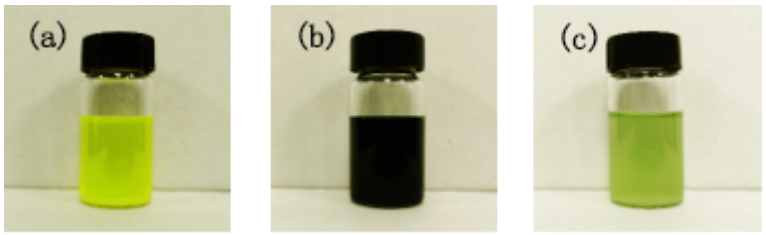

Figure 6

The color change of PMo12 at redox process: a WS-PMo12 solution before heating; b WS-PMo12 solution after heating; c PMo12 solution after electrolysis.